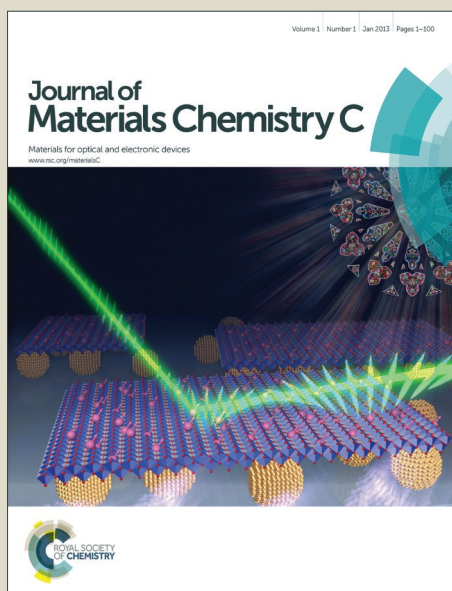


Journal of Materials Chemistry C

Accepted Manuscript



This is an *Accepted Manuscript*, which has been through the Royal Society of Chemistry peer review process and has been accepted for publication.

Accepted Manuscripts are published online shortly after acceptance, before technical editing, formatting and proof reading. Using this free service, authors can make their results available to the community, in citable form, before we publish the edited article. We will replace this *Accepted Manuscript* with the edited and formatted *Advance Article* as soon as it is available.

You can find more information about *Accepted Manuscripts* in the [Information for Authors](#).

Please note that technical editing may introduce minor changes to the text and/or graphics, which may alter content. The journal's standard [Terms & Conditions](#) and the [Ethical guidelines](#) still apply. In no event shall the Royal Society of Chemistry be held responsible for any errors or omissions in this *Accepted Manuscript* or any consequences arising from the use of any information it contains.



ARTICLE

Bismuth-catalyzed and doped p-type ZnSe nanowires and their temperature-dependent charge transport properties

Received 00th January 20xx,
Accepted 00th January 20xx

Xiwei Zhang,^{a,b} Jiansheng Jie,^{*b} Xiujuan Zhang,^b Fengjun Yu^a

DOI: 10.1039/x0xx00000x

www.rsc.org/

Au catalysts have been found to diffuse into semiconductor nanostructures and form non-radiative recombination centers during the synthesis process. This adverse impact to p-type doping of ZnSe nanostructures is even more together with its self-compensation effect. Herein, low melt-point Bi is used as catalysts for the synthesis of p-ZnSe nanowires *via* VLS mechanism while the incorporation of Bi catalyst atoms causes effective p-type doping in the as-grown nanostructures. Top-gate MISFETs are fabricated to confirm the p-type conduction of the Bi-catalyzed and doped ZnSeNWs. Temperature-dependent electrical measurements are used for understanding the charge transport mechanism and doping effect of semiconductors. Thermal activation behavior of carriers is considered to be the dominator in the temperature range of 150–300K while 3D Mott VRH mechanism is considered to prevail over other mechanism at lower temperature range of 50–140K.

Introduction

As a wide band-gap II-VI semiconductor, ZnSe has attracted a great deal of attentions because it can offer extensive applications in optoelectronic devices such as light-emitting diodes (LEDs), laser diodes (LDs) and solar cells.^{1–3} Recently, ZnSe nanostructures have been paid attention by many investigators due to their unique optical and electrical properties in small scale^{4,5}. Their synthesis and characteristics have been intensively studied.^{6–8} In spite of these progresses, the practical applications of the ZnSe nanostructures are still hampered by the difficulties in controlling their transport properties, especially for their p-type conductivity. Owing to self-compensation effect, efficient p-type doping in ZnSe films and bulks is hindered.⁹ However, recent investigations have demonstrated that efficient p-type doping in ZnSe nanostructures could be achieved by using group V elements as the dopants, such as phosphorus (P), bismuth (Bi) and arsenic (As).^{10–12} The high-crystal quality and the potential size effect are suggested to be responsible for the improved doping performance in ZnSe nanostructures.¹³

Until now, Au is considered to be the dominant catalyst metal for semiconductor nanostructures *via* VLS mechanism, owing to its chemical inertness, thermal stability and the ability to form a eutectic alloy at low temperature.¹⁴ But Au has been found to

diffuse into semiconductor nanostructures and form non-radiative recombination centres that greatly deteriorate electrical and optical properties.^{15,16} It is important to develop suitable alternative metal catalysts to solve the above problems. Low-melting-point metals such as indium (In), tin (Sn), gallium (Ga) and bismuth (Bi) are primary candidates.^{17–21}

Yu and co-workers have demonstrated that Bi could catalyze the growth of Si nanowires (SiNWs) *via* VLS mechanism while the incorporation of Bi catalyst atoms could cause effective n-type doping in the as-grown SiNWs.²² Their achievement means that catalysis and doping could be achieved in one step by the same metal during the growth of semiconductor nanostructures. It will provide a new platform to synthesize high quality nanostructures if this strategy could be popularized to the growth of other semiconductor nanostructures, with the advantages of avoiding deep-level defects induced by Au and simplifying the growth process by omitting Au film deposition on the Si substrate.

To further promote and exploit semiconductor nanostructures in electronic and optoelectronic applications, a deeper understanding of their charge transport properties is necessary. Hopping conduction is an important charge transport mechanism at low temperature^{23–25} and has been extensively studied on many low-dimension semiconductor nanostructures,^{26–28} such as Mn-doped ZnO nanowires, FeS₂ Nanorods/nanobelts, SnO₂ nanobelts and Mn Ion-Implanted GaAs Nanowires. The conductance of carriers is deemed to be controlled by the hopping of holes/electrons between localized states nearby the Fermi level due to most of the free holes/electrons are recaptured by the acceptors/donors at sufficiently low temperatures. Furthermore, it is considered to be the case of Mott variable-range hopping (Mott–VRH) when the Coulomb interaction of the electrons can be neglected.²⁹ In this case, direct holes/electrons hopping between acceptors/donors in the impurity band provides the main contribution to the

^a College of physics and electrical engineering, Anyang Normal University, Anyang Henan 455000, P. R. China

^b Institute of Functional Nano & Soft Materials (FUNSOM), Collaborative Innovation Center of Suzhou Nano Science and Technology, Jiangsu Key Laboratory for Carbon-Based Functional Materials & Devices, Soochow University, Suzhou, Jiangsu 215123, P. R. China.

*Email: jsjie@suda.edu.cn

† Footnotes relating to the title and/or authors should appear here.

Electronic Supplementary Information (ESI) available: [details of any supplementary information available should be included here]. See DOI: 10.1039/x0xx00000x

conductivity.³⁰ To our best knowledge, there have been no reports on this charge transport mechanism of ZnSe nanowires (ZnSeNWs).

Herein, simultaneous ZnSe nanowires growth and p-type doping were realized in one step by using Bi as the catalysts and dopants *via* chemical vapour deposition. Top-gate MISFETs were fabricated to conduct their electrical and charge transport properties. Furthermore, temperature-dependent electrical measurements were conducted in the range of 50–300K. Thermal activation behaviour of carrier is considered to be the dominator in the temperature range of 150–300K while 3D Mott VRH mechanism is considered to prevail over other mechanism at lower temperature range of 50–140K.

Experiments

ZnSe nanowires were synthesized by chemical vapour deposition in a horizontal alumina tube furnace. In a typical experiment, an alumina boat filled with 0.3g ZnSe powder (Aldrich, 99.99%) was transferred to the center region of the furnace, as well as another boat loaded up with 0.1g Bi powder (Aladdin, 99.99%) was placed at about 10 cm upstream away from the center. Instead of Si substrates coated with 5–10 nm Au film, long bare Si substrates (~5cm) cleaned by diluted HF, acetone and DI water were put at the ~15 cm downstream away from the center. The reaction chamber was first evacuated to a base pressure of 5×10^{-3} Pa and then filled with mixture gas of Ar and H₂ (5% in volume) at a constant flow rate of 80 sccm. The pressure in the tube was adjusted and maintained to 100 Torr before the center region of the furnace was heated to 1050 °C. During the growth process, the temperature of the boats filled with Bi powder and long Si substrates (5 cm) were kept at the range of 600 – 800 °C and 300 – 700 °C, respectively. After the growth process, the furnace was cooled down to room temperature and the samples were taken out of the furnace.

Morphologies and structures of the as-synthesized ZnSeNWs were characterized by filed-emission scanning electron microscopy (FESEM, SIRION 200 FEG) and high-resolution transmission electron microscopy (HRTEM, JEOL JEM-2010). Compositions were analyzed by X-ray photoelectron spectroscopy (XPS, Thermo ESCALAB 250) and energy dispersive X-ray spectroscopy (EDS).

To assess the electrical properties of as-synthesized ZnSeNWs, top-gate metal-insulator-semiconductor field effect transistors (MISFETs) based on single ZnSeNW were constructed. Firstly, the ZnSeNWs were dispersed on a SiO₂ (300 nm)/p⁺-Si substrate, followed by photolithography and lift-off processes to define Au (50 nm) source/drain electrodes on the ends of ZnSeNWs. Then, a thin layer of Si₃N₄ (50 nm) gate dielectric was deposited by magnetron sputtering and another 50 nm Au electrode was fabricated above the Si₃N₄ layer as gate electrodes. Four electrode devices used to demonstrate good Ohmic contact between Au and p-type ZnSeNWs were also fabricated by photolithography and lift-off processes. Fast annealing process in Ar atmosphere was carried out at 550 °C for 5 min after the deposition of Au source/drain electrodes in order to activate Bi acceptors in ZnSeNW.¹¹ Another fast annealing process at 350 °C for 5 min was used to reduce the leakage current in Si₃N₄ dielectric layer. The properties of MISFETs were measured by using a

semiconductor characterization system (Keithley 4200-SCS) while temperature-dependent electrical measurements were carried out by using a low temperature probe station.

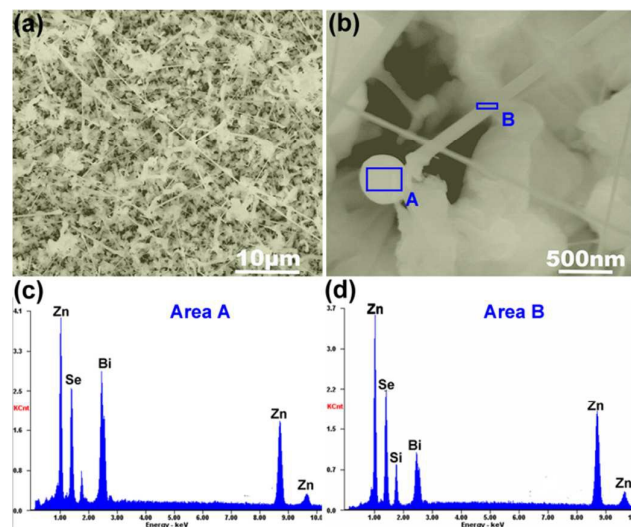


Fig. 1 (a) Typical SEM image of as-synthesized ZnSeNWs in a certain area of the Si substrate. (b) An enlarged SEM image of individual ZnSeNW. (c) EDS spectrum of Area A (Bi catalyst tip) in Fig. 1b. (d) EDS spectrum of Area B (ZnSeNW part) in Fig. 1b.

Results and discussions

Fig. 1a shows the typical FESEM image of as-synthesized ZnSeNWs in a certain area of the Si substrate. It is seen that the NWs have uniform morphology and sizes with diameter in the range of 100 – 300 nm and length from dozens of micrometers to several hundreds of micrometers. Unlike dense NWs synthesized by Au catalyst in reported works,^{31–33} the NWs here with sparse and underneath particles are observed. The particles are Bi, which were deposited on Si substrates before NWs growth due to its much lower melting point (271 °C) than ZnSe (1520 °C). The enlarged SEM image of individual ZnSeNW is shown in Fig. 1b. In which, large catalyst particle on the top of the straight NW is clearly observed. Further composition analysis of the catalyst particle and the NW were carried out by EDS and shown in Fig. 1c and 1d. Strong Bi signal is observed in area A (the catalysts part) while strong Zn and Se peaks are observed in the NW part (area B). It is important to note that Si, Zn, Se and Bi peaks were all detected in area A and B owing to background signals and instrument precision. Further EDS analysis in HRTEM is much more pure and accurate as shown in the next parts.

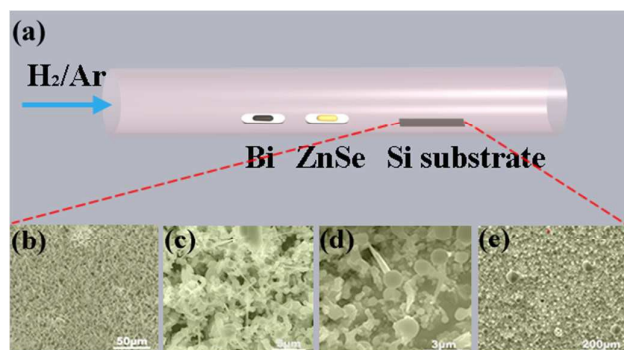


Fig. 2 (a) Schematic illustration of the furnace tube for Bi-catalyzed ZnSeNWs growth. SEM images of products on a typical Si substrate with a length of ~ 5 cm from near to far to the center region of the furnace, in order of (b), (c), (d) and (e).

ZnSe nanostructures with different morphologies along the Si substrate surface were obtained due to the temperature gradient (Fig. 2). At the far-end of the substrate (low temperature region), high density of Bi particles, rather than ZnSeNWs, is observed (Fig. 2e). In the middle part with a higher temperature, tail-like and wire-like ZnSe nanostructures with large Bi heads were synthesized as shown in Fig. 2d and 2c. That is to say, ZnSeNWs with large catalyst tips, uniform morphology and sizes could be formed in the middle part of Si substrate with comfortable temperature. However, if the temperature gets too high, rod-like ZnSe structures without any sign of Bi catalysts (Fig. 2b) would be synthesized at the near-end of the substrate. These rod-like ZnSe structures are considered as grown by self-catalytic action of Zn.²¹ Generally speaking, a narrow region (<1 cm) on the substrate is deemed to be suitable for the synthesis of Bi-catalyzed ZnSeNWs. Moreover, Bi catalysts with larger diameters than that of NWs are considered to be the similarity of other low melting point catalysts.^{34,35}

The growth process of ZnSe nanostructures can be explained by the Vapor-Liquid-Solid (VLS) mechanism. When the temperature goes up, Bi powder would be firstly evaporated and transported by carrier gas owing to its lower melting point. Then, Bi vapor will be brought to low temperature region and deposit on the bare Si substrate as liquid droplets. When the temperature is enough to vaporize ZnSe, Zn and Se vapor will be brought to the low temperature region by carrier gas too. At the far-end of the substrate, the temperature is lower than the solid/liquid phase transition temperature of Bi-Zn alloy (440 °C). Thus, it is unfavorable to the dissolution of Zn in Bi catalysts. As a result, only Bi particles are deposited. In the middle part of substrate with comfortable temperature, Zn and Se vapor would be absorbed by the Bi droplets and separated out when the alloy droplets reach supersaturation. At last, continuous absorption and separation could result in the ZnSeNWs growth along a direction. At the near-end of the substrate, molten Zn, rather than Bi, will deposit due to the high temperature. The molten Zn not only acts as the reactant but also provides an energetically favoured site for the absorption of Se. Continual feeding of Zn and Se into the molten Zn results into the formation of the rod-like ZnSe structures. Thus, self-catalytic VLS mechanism is considered to play an important role in the ZnSe nanostructure growth at the near-end.

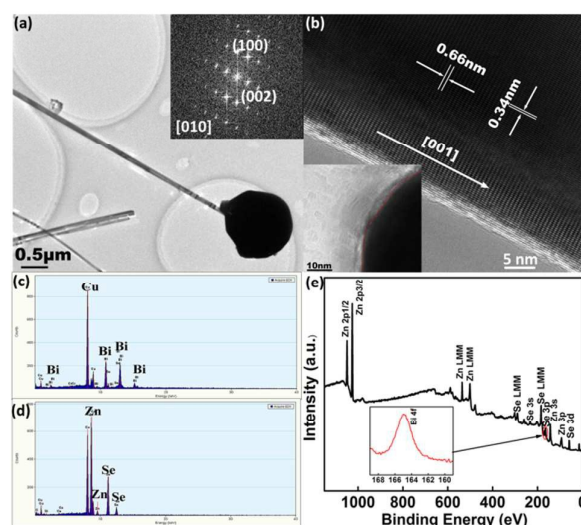


Fig. 3 (a) TEM image of a single ZnSeNW with a large catalyst tip. Inset shows the corresponding FFT pattern. (b) HRTEM image of the ZnSeNW. Inset shows the HRTEM image which depicts the boundaries between ZnSeNWs and Bi catalyst with red dashed lines. (c) EDS spectrum taken from Bi catalyst tip. (d) EDS spectrum taken from the ZnSeNW part. Cu peaks come from the Cu grid used for TEM investigation. (e) XPS spectrum of the ZnSeNWs. Inset shows the XPS peak that originated from Bi in ZnSeNWs.

TEM and XPS analysis in Fig. 3 are used to confirm the topography, structures, crystal quality and compositions of the as-synthesized ZnSeNWs. A single NW with a much larger Bi catalyst tip is shown in Fig. 3a, which indicates that Bi-catalyzed ZnSeNWs have smooth surface and uniform diameter. HRTEM image shown in Fig. 3b and the corresponding fast fourier transform (FFT) shown in the inset in Fig. 3a depict that the NWs are single-crystal wurtzite structure with a grown orientation of [001]. Close-up view of the catalyst/NW interface is shown in the inset in Fig. 3b. It should be noted that obvious boundary between ZnSeNWs and Bi catalyst could be identified by their different crystalline structures and contrast. Further EDS characterization shown in Fig. 3c and 3d indicate that only Bi and Cu signals are detected in the catalyst tips while pure Zn and Se are identified in the NWs part. The TEM characterization are in keeping with the former analysis by SEM system and confirm that Bi-catalyzed ZnSeNWs have the same uniform morphology and high crystal quality as ZnSeNWs that are catalyzed by Au catalysts. Bi is considered to be an efficient p-type dopant for II-VI semiconductors and has been demonstrated in our previous work.¹¹ While Bi works as catalysts, it is also supposed to diffuse into the NWs and achieve *in situ* doping during the growth of ZnSeNWs. XPS measurements were used to detect the compositions of ZnSeNWs and the XPS spectrum is shown in Fig. 3e. The two Zn peaks centered at 1026 eV and 1049 eV corresponding to Zn $2p_{3/2}$ and Zn $2p_{1/2}$ are attributed to Zn-Se bonding. Moreover, a weak peak at ~ 165 eV corresponding to Bi $4f$ core level emission is considered to result from Bi-Se bonding. The XPS analysis implies that the Bi element has been successfully incorporated into the ZnSeNWs. However, we note that the peaks located at 157.0 eV and

below 157.0 eV that correspond to isolated Bi and Bi–Zn bonding do not appear in the XPS spectrum, implying that the Bi_{Se} (Bi occupying Se site) and Bi_i (interstitial atom) defects are absent in the ZnSeNWs. That is to say, most of the Bi that is incorporated into the ZnSeNWs should exist as Bi occupy Zn site (Bi_{Zn}) rather than Bi_{Se} or Bi_i. The reason may be that Bi has a lower electronegativity (2.02 eV) than Se (2.55 eV), which makes it easier to occupy the Zn antisite instead of substituting the Se atom. But, Bi_{Zn} is a metastable state due to its configuration with a large lattice relaxation and is inclined to form Bi-related complexes with other defects. On the other hand, Bi is a large-size-mismatched dopant for ZnSe because of its larger ion radius (1.63 Å), and tends to induce nearby Zn vacancies in ZnSeNWs. As a result, the complexes of Bi occupy Zn site and two Zn vacancies (Bi_{Zn}-2V_{Zn}) with low formation energy and shallow acceptor level are considered to be the most probable acceptor defects in Bi-catalyzed and doped ZnSeNWs.^{11,36}

The composition analysis demonstrates that Bi could diffuse into the NWs and achieve *in situ* doping when it works as catalysts for the growth of ZnSeNWs. Compared with arsenic (As) and antimony (Sb) doped ZnSeNWs realized by Song and Nie,^{12,33} the usage of Bi offers the following advantages: i) Bi-doped ZnSe is friendly to environmental and has wider applications because of Bi's less toxic. ii) Bi has a low melting temperature of 271 °C and low solubility in most semiconductors. It is a possible candidate for alternative catalysts. iii) Bi-related defect complexes can introduce shallow acceptor levels in ZnSe nanostructure. iv) Catalysis and doping could be simultaneously achieved by Bi during the growth of ZnSeNWs, which could simplify the growth process and avoid non-radiative recombination centers induced by conventional Au catalyst.

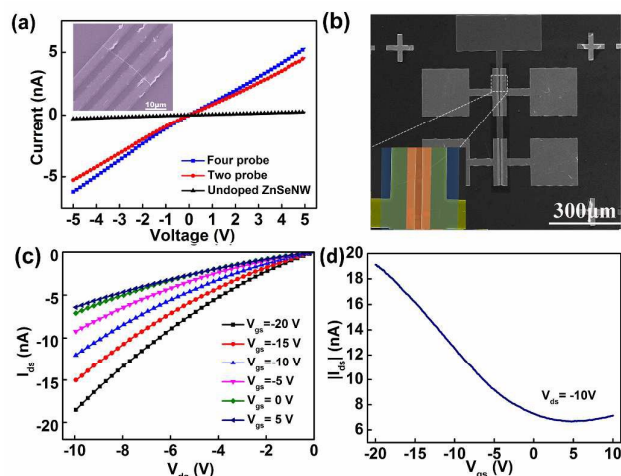


Fig. 4 (a) I - V curves of an undoped ZnSeNW and a single Bi-doped ZnSeNW by using two probe and four probe methods at room temperature. Inset shows an SEM image of a NW with contacts for 4-point resistance measurements. (b) SEM image of a typical top-gate MISFET based on individual ZnSeNW. Inset shows the enlarged FESEM of the nanowire region. (c) The gate dependent I_{ds} - V_{ds} curves of a typical MISFET. (d) $|I_{ds}|$ - V_{gs} curve of the same MISFET.

Electrical and charge transport properties of Bi-catalyzed and doped ZnSeNWs are investigated to confirm the doping effect. Fig. 4a shows current-voltage (I - V) curves of an undoped ZnSeNW and a

single Bi-doped ZnSeNW by using two probe and four probe methods at room temperature. From the measurements we can conclude that the Bi-catalyzed and doped ZnSeNW has a higher conductance than that of undoped ZnSeNW and a low contact resistance with Au electrodes. Fig. 4b depicts the SEM image of a typical top-gate MISFET based on individual ZnSeNW. The gate dependent source-drain current (I_{ds}) versus source-drain voltage (V_{ds}) curves measured at varied gate voltage (V_{gs}) from -20 V to +5 V are shown in Fig. 4c. The $|I_{ds}|$ - V_{gs} curve is shown in Fig. 4d. It is found that $|I_{ds}|$ decreases with the increase of V_{gs} , which means that the conduction of the ZnSeNW decreases when V_{gs} increases. The feature is consistent with the typical characteristic of p-channel transistors, revealing the p-type conduction of the Bi-catalyzed and doped ZnSeNWs. Furthermore, the hole mobility μ_h and carrier concentration n_h are deduced to be $\sim 2.86 \times 10^{-2} \text{ cm}^2 \text{ s}^{-1} \text{ V}^{-1}$ and $3.97 \times 10^{17} \text{ cm}^{-3}$, respectively, according to the following equations:

$$\mu_h = L g_m \frac{\ln(1 + 2h/d)}{2\pi\epsilon_0\epsilon_{Si_3N_4} V_{ds}} \quad (1)$$

$$g_m = \frac{dI_{ds}}{dV_{gs}} \quad (2)$$

$$n_h = \sigma / q\mu_h \quad (3)$$

where L , h and d represent the NW channel length (8 μm), gate dielectric layer thickness (50 nm) and the NW diameter (~ 200 nm). $\epsilon_{Si_3N_4}$ is the dielectric constant (7.5) of the dielectric layer and g_m is the transconductance which is extracted from the linear regime of I_{ds} - V_{gs} curve. In addition, σ is the conductivity of a single NW which is obtained to be $\sim 1.82 \times 10^{-3} \text{ Scm}^{-1}$.

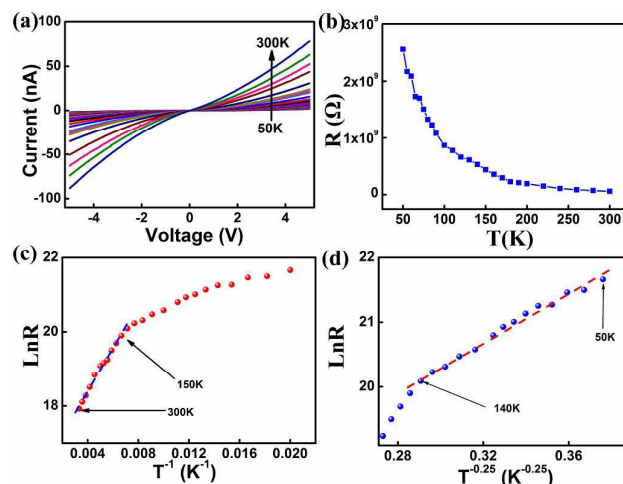


Fig. 5 (a) The temperature-dependence I - V curves, (b) The resistance versus temperature (R - T) curve, (c) $\text{Ln}R$ versus T^{-1} curve and (d) $\text{Ln}R$ versus $T^{-0.25}$ curve of a typical device in the range of 50–300K.

Temperature-dependent electrical measurement is significant to understand the charge transport mechanism and doping effect of semiconductors. Therefore, temperature-dependent electrical measurements of Bi-catalyzed and doped ZnSeNWs were conducted in the temperature range of 50–300K. The temperature-dependent I - V curves of the p-type ZnSeNWs and the resistance

versus temperature (R - T) curve are shown in Fig. 5a and 5b. It is seen that the resistance of the NWs decreases dramatically with the rising of temperature from 50K to 300K. Detailed analysis indicates that the charge transport is governed by different mechanisms in different temperature ranges. When the temperature is higher than 150 K, $\ln R$ versus T^{-1} curve (Fig. 5c) performs a linear fitting. This behaviour is in good agreement with the thermal activation of carriers:

$$R_{(T)} = R_0 \exp\left(\frac{\Delta E}{k_B T}\right) \quad (4)$$

where R_0 is a temperature-independent constant, k_B is the Boltzmann constant and ΔE is the activation energy. By fitting the linear curve in the range of 150 – 300K, an activation energy of $\Delta E = 54.3$ meV is obtained, which indicates that the Bi-related acceptor level located 54.3 meV above the valence band. It should be noted that the activation energy here is lower than that of p-type ZnSe film and nanostructures doped by other V group elements (Supporting Information, Table. S1). The above analysis demonstrates that $\text{Bi}_{\text{Zn}}\text{-}2\text{V}_{\text{Zn}}$ complexes are shallow acceptors and easy to activate. Therefore, Bi is considered as an efficient p-type dopant in ZnSe nanostructures.

Further investigation of the relation between $\ln R$ and $T^{-0.25}$ is shown in Fig. 5d. A linear relationship in this plot in the temperature range of 50-140K is found, which indicates that the resistance as a function of temperature at lower temperature region follows the relation predicted by Mott variable range hopping (VRH) mechanism:³⁷

$$R_{(T)} = R_0 \exp\left(\frac{T_0}{T}\right)^{\frac{1}{n+1}} \quad (5)$$

where $n=1, 2$, or 3 for one-dimension (1D), 2D or 3D system, respectively. R_0 is a prefactor and T_0 is the characteristic temperature, which are both independent on the temperature. Herein, n is defined as 3 for Bi-catalyzed and doped p-type ZnSeNWs, and the mechanism is considered as 3D Mott VRH. Furthermore, T_0 is related to the hole localization length (α) and density of states near the Fermi level $N(E_F)$ according to

$$T_0 = 18/k_B \alpha^3 N(E_F) \quad (6)$$

From the slope of the linear fit to $\ln R$ and $T^{-0.25}$ curve in Fig. 5d, we deduce a value of $T_0 = 1.28 \times 10^5$ K, which corresponds to a $N(E_F) = 6.37 \times 10^{20}$ (eV \cdot cm 3) $^{-1}$. The value of α is assumed to be of the same order as the acceptor Bohr radius (1 nm). Mott VRH is the mechanism to describe the conductance of carriers which is considered to be controlled by the hopping of electrons/holes between localized states nearby the Fermi level at low temperature. Consequently, the high density of states near the Fermi level can efficiently increase the hopping probability of Bi-doped ZnSeNWs at low temperature.³⁸ For p-type ZnSeNWs, most of the holes are recaptured by the impurity energy levels at very low temperature, and hole-conduction in the valence band becomes subordinate. As a result, direct hole hopping between acceptors in the impurity band provides the main contribution to the conductance.³⁹ A hopping hole will always try to jumping from occupied acceptors to empty ones by using the lowest activation energy (ΔE_h) and shortest hopping distance (r). There is an

optimum r which could maximize the hopping probability and consequently govern the hopping conduction. The hopping distance is temperature dependent and is defined as:

$$r = \left[\frac{9\alpha}{8\pi k_B T N(E_F)} \right]^{\frac{1}{4}} \quad (7)$$

r is calculated to be ~ 2.67 nm at 50 K, which is much smaller than diameter (200 nm) of Bi-catalyzed and doped ZnSeNWs in this paper and indicates that the hopping conduction could also happen in the radius direction of the NWs. Therefore, it is defined as 3D Mott VRH here. In addition, the remarkable 3D VRH hopping conduction of Bi-doped ZnSeNWs at low temperature means that Bi-related complexes ($\text{Bi}_{\text{Zn}}\text{-}2\text{V}_{\text{Zn}}$) could introduce a high density of states near the Fermi level. However, more detailed investigations are needed to unravel the hopping processes through the Bi-related impurity band influenced by these impurity states in the future work.

Conclusions

Low-melt-point Bi was first used as catalysts for the synthesis of ZnSe nanowires *via* VLS mechanism in this work. The incorporation of Bi catalyst atoms during synthesis can introduce Bi-related defect complexes ($\text{Bi}_{\text{Zn}}\text{-}2\text{V}_{\text{Zn}}$) in ZnSe nanowires and form shallow acceptor level. This simultaneous ZnSe nanowires growth and p-type doping method is considered to simplify the growth process and avoid non-radiative recombination centers induced by conventional Au catalyst. The doping effect and charge transport properties were further investigated by electrical measurements. Remarkable p-type conduction and low activation energy of ~ 54.3 meV induced by Bi-related defect complexes were confirmed. Even more important, 3D VRH hopping conduction of Bi-doped ZnSeNWs is investigated and reveals their charge transport mechanism at low temperature. Our results demonstrate a new growth/doping method which would be an important platform for the synthesis semiconductor nanostructures.

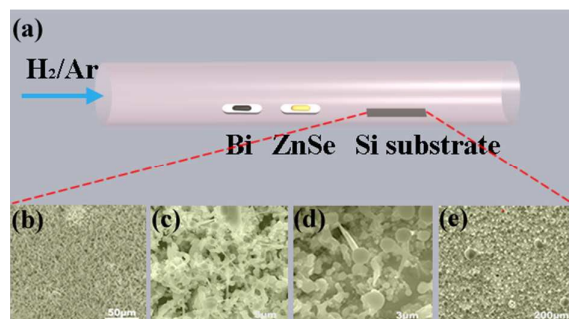
Acknowledgements

This work was supported by the National Natural Science Foundation of China (Nos. 51402004, 61422403, 51172151), the National Basic Research Program of China (Nos. 2013CB933500) and the Science and Technology Development Project of Henan province (Nos. 152102210293 and 15A510006).

Notes and references

- 1 J. Ren, K. A. Bowers, B. Sneed, D. L. Dreifus, J. W. Cook and J. F. Schetzina, *Appl. Phys. Lett.*, 1990, **57**, 1901.
- 2 M. A. Haase, J. Qiu, J.M. DePuydt and H. Cheng, *Appl. Phys. Lett.*, 1991, **59**, 1272.
- 3 P. Mahawela, G. Sivaraman, S. Jeedigunta, J. Gaduputi, M. Ramalingam and S. Subramanian, *Mater. Sci. Eng.B*, 2005, **116**, 283.

- 4 A. Saxena, S. Yang, U. Philipose, and H. E. Ruda, *J. Appl. Phys.*, 2008, **103**, 053109.
- 5 Z. Wang, J. S. Jie, F. Z. Li, L. Wang, T. X. Yan, L. B. Luo, B. Nie, C. Xie, P. Jiang, X. W. Zhang, Y. Q. Yu, C. Y. Wu, *ChemPlusChem*, 2012, **77**, 470-475.
- 6 X. T. Zhang, Z. Liu, Y. P. Leung, Q. Li and S. K. Hark, *Appl. Phys. Lett.*, 2003, **83**, 5533.
- 7 S. L. Xiong, B. J. Xi, C. M. Wang, G. C. Xi, X. Y. Liu and Y. T. Qian, *Chem. Eur. J.*, 2007, **13**, 7926.
- 8 Y. P. Leung, W. C. H. Choy, I. Markov, G. K. H. Pang, H. C. Ong and T. I. Yuk, *Appl. Phys. Lett.*, 2006, **88**, 183110.
- 9 D. B. Laks and C. G. Van de Walle, *Phys. B*, 1993, **185**, 118.
- 10 X. W. Zhang, X. J. Zhang, X. Z. Zhang, Y. P. Zhang, L. Bian, Y. M. Wu, C. Xie, Y. Y. Han, Y. Wang, P. Gao, L. Wang, J. S. Jie, *J. Mater. Chem.*, 2012, **22**, 22873-22880.
- 11 X. W. Zhang, J. S. Jie, Z. Wang, C. Y. Wu, L. Wang, Q. Peng, Y. Q. Yu, P. Jiang and C. Xie, *J. Mater. Chem.*, 2011, **21**, 6020.
- 12 H. S. Song, W. J. Zhang, G. D. Yuan, Z. B. He, W. F. Zhang, Y. B. Tang, L. B. Luo, C. S. Lee, I. Bello and S. T. Lee, *Appl. Phys. Lett.*, 2009, **95**, 033117.
- 13 J. S. Jie, W. J. Zhang, I. Bello, C. S. Lee and S. T. Lee, *Nano Today*, 2010, **5**, 313.
- 14 P. Nguyen, H. T. Ng, M. Meyyappan, *Adv. Mater.*, 2005, **17**, 1773.
- 15 V. Schmidt, J. V. Wittermann, S. Senz, U. Gosele, *Adv. Mater.*, 2009, **21**, 2681.
- 16 J. E. Allen, E. R. Hemesath, D. E. Perea, J. L. Lensch-Falk, Z. Y. Li, F. Yin, M. H. Gass, P. Wang, A. L. Bleloch, R. E. Palmer, L. J. Lauhon, *Nat. Nanotechnol.*, 2008, **3**, 168.
- 17 Z. W. Wang and Z. Y. Li, *Nano Lett.*, 2009, **9**, 1467-1471.
- 18 G. Mi, L. K. Li, Y. B. Zhang and G. F. Zheng, *Nanoscale*, 2012, **4**, 6276-6278.
- 19 I. Zardo, L. Yu, S. Conesa-Boj, S. Estrade, P. J. Alet, J. Rossler, M. Frimmer, P. Roca i Cabarrocas, F. Peiro, J. Arbiol, J. R. Morante, A. Fontcuberta i Morral, *Nanotechnology*, 2009, **20**, 155602.
- 20 C. Y. Yan and P. S. Lee, *J. Phys. Chem. C*, 2009, **113**, 2209.
- 21 S. R. Moon, J. H. Kim, and Y. Kim, *J. Phys. Chem. C*, 2012, **116**, 10368-10374.
- 22 L. W. Yu, F. Fortuna, B. O'Donnell, T. Jeon, M. Foldyna, G. Picardi, and P. Roca i Cabarrocas, *Nano Lett.*, 2012, **12**, 4153-4158.
- 23 N. F. Mott, E. A. David, *Electronic Processes in Noncrystalline Materials*, Oxford University Press, Oxford, 1979.
- 24 B. I. Shklovskii, A. L. Efros, *Electronic Properties of Doped Semiconductors*, Springer, Berlin, 1979.
- 25 Y. J. Ma, Z. Zhang, F. Zhou, L. Lu, A. Z. Jin and C. Z. Gu, *Nanotechnology*, 2005, **16**, 746-749.
- 26 J. P. Han, M. R. Shen, and W. W. Cao, *Appl. Phys. Lett.*, 2003, **82**, 67-69.
- 27 M. Caban-Acevedo, D. Liang, K. S. Chew, J. P. DeGrave, N. S. Kaiser, and S. Jin, *ACS Nano*, 2013, **7**, 1731-1739.
- 28 E. R. Viana, J. C. Gonzalez, G. M. Ribeiro and A. G. de Oliveira, *physica status solidi (RRL)*, 2012, **6**, 262-264.
- 29 Y. J. Ma, F. Zhou, L. Lu, Z. Zhang, *Solid State Communications*, 2004, **130**, 313-316.
- 30 L. B. Huang, D. D. Li, P. C. Chang, S. Chu, H. Bozler, I. G. S. Beloborodov and J. G. Lu, *Phys. Rev. B*, 2011, **83**, 245310.
- 31 Y. Jiang, X. M. Meng, J. Liu, Z. Y. Xie, C. S. Lee, S. T. Lee, *Adv. Mater.*, 2003, **15**, 323-327.
- 32 M. Lin, T. Sudhiranjan, C. Boothroyd, K. P. Lo, *Chemical Physics Letters*, 2004, **400**, 175-178.
- 33 B. Nie, L. B. Luo, J. J. Chen, J. G. Hu, C. Y. Wu, L. Wang, Y. Q. Yu, Z. F. Zhu and J. S. Jie, *Nanotechnology*, 2013, **24**, 095603.
- 34 P. X. Gao and Z. L. Wang, *J. Phys. Chem B*, 2004, **108**, 7534.
- 35 Z. W. Wang, Z. Y. Li, *Nano Lett.*, 2009, **9**, 1467.
- 36 Y. Q. Shen, N. Xu, W. Hu, X. F. Xu, J. Sun, Z. F. Ying, J. F. Wu, *Solid-State Electronics*. 2008, **52**, 1833-1836.
- 37 J. Li, H. Z. Zhong, H. J. Liu, T. Y. Zhai, X. Wang, M. Y. Liao, Y. Bando, R. B. Liu and B. S. Zou, *J. Mater. Chem.*, 2012, **22**, 17813-17819.
- 38 N. F. Mott, *Phil. Mag.*, 1969, **19**, 835.
- 39 W. Paschoal, Jr., S. Kumar, C. Borschel, P. Wu, C. M. Canali, C. Ronning, L. Samuelson and H. Pettersson, *Nano Lett.*, 2012, **12**, 4838-4842.



Simultaneous ZnSe nanowires growth and p-type doping is realized in one step by using Bi as the catalysts and dopants *via* chemical vapor deposition. Top-gate MISFETs are fabricated to confirm the p-type nature of the as-synthesized ZnSeNWs. Temperature-dependent electrical measurements are used for understanding the charge transport mechanism and doping effect.